Revista Internacional de Investigación e Innovación Tecnológica

Página principal: www.riiit.com.mx

Optimization of steel surface preparation for the fabrication of coating thickness reference materials

Optimización de la preparación de la superficie de acero para la fabricación de materiales de referencia de espesores de recubrimientos

Domínguez-García, A.[a], Mercader-Trejo, F.E.[b], Mondragón-Rodríguez, G.C.[a]*, Guzmán-Tapia, M.[a], Herrera-Basurto, R.[cd]*

[a] Dirección de Tecnologías Estratégicas y Posgrado, Centro de Ingeniería y Desarrollo Industrial, Querétaro, México.
[b] Posgrado e Investigación, Universidad Politécnica de Santa Rosa Jáuregui. Querétaro, México.
[c] Dirección de Innovación y Negocios, Total Metrology in Chemistry, Querétaro, México.
[d] Instituto Tecnológico Nacional, Dirección de Posgrado, sede Morelia, México.
a.dominguez@posgrado.cidesi.edu.mx; fmercader@upsrj.edu.mx; guillermo.mondragon@cidesi.edu.mx*; manuel.guzman@cidesi.edu.mx; raul.herrera@tmicnet.com*

Technological innovation: Effect of substrate properties on the quality of coatings.

Industrial application area: Metrology, coating quality, surface engineering, materials.

Received: July 11th, 2024
Accepted: August 26th, 2024

Abstract

The quality of the coating depends on the quality of the substrate surface preparation. It is often believed that achieving a mirror finish on metallic substrates is sufficient to obtain a uniform coating or having a rough surface is synonymous with better adhesion. However, both of them, are paradigms. Currently, there is neither a clear definition of the term "mirror finish" nor sufficient information to quantitatively determine the quality of a surface suitable to receive a coating with the following characteristics: homogeneous, stable and uniform. This article presents a procedure designed and implemented to obtain an ad hoc surface (mirror finish) on an AISI M2 metallic substrate, as well as a test bench to know the characteristics of the prepared surface and to see the compatibility and coherence of the substrate and the coating to achieve the properties of a thickness pattern in a coating. The evaluation of brightness according to roughness from 0.04 to 0.08 µm and some of the defect results are as follows; pores from 0.10 to 1.00 µm, scratches from 0.30 to 10.00

µm, then the crystal structure was checked for the substrate and coating, FCC and HC respectively. Therefore, there is coherence in the substrate-coating system. Additionally, the hardness measuring indicated that the substrate is harder than the coating, this will favor adhesion between both of them.

Keywords: Coherence structural, Mirror finish, Standard, Surface defects.

Resumen

La calidad del recubrimiento depende de la calidad de la preparación de la superficie del sustrato. A menudo se cree que lograr un acabado de espejo en sustratos metálicos es suficiente para obtener un recubrimiento uniforme o que tener una superficie rugosa es sinónimo de mejor adherencia. Sin embargo, ambos son paradigmas. Actualmente, no existe una definición clara del término "acabado espejo" ni información suficiente para determinar cuantitativamente la calidad de una superficie apta para recibir un recubrimiento con las siguientes características: homogénea, estable y uniforme. Este artículo presenta un procedimiento diseñado e implementado para obtener una superficie ad hoc (acabado espejo) sobre un sustrato metálico AISI M2, así como un banco de pruebas para conocer las características de la superficie preparada y ver la compatibilidad y coherencia del sustrato y el recubrimiento para conseguir las propiedades de un patrón de espesor en un recubrimiento. La evaluación del brillo según la rugosidad de 0.04 a 0.08 µm y algunos de los resultados de los defectos son los siguientes; poros de 0.10 a 1.00 µm, arañazos de 0.30 a 10.00 µm, después se comprobó la estructura cristalina para el sustrato y el revestimiento, FCC y HC respectivamente. Por lo tanto, existe coherencia en el sistema sustrato-recubrimiento. Además, la medición de la dureza indicó que el sustrato es más duro que el recubrimiento, lo que favorecerá la adhesión entre ambos.

Palabras clave: Acabado espejo, Coherencia estructural, Defectos superficiales, Estándar,

I. Introduction

In recent years, significant advances in industry and research have led to an increasing demand for advance materials with exceptional mechanical properties and high-quality surface finishes (Heng et al., 2017). To achieve these objectives, researchers such as Cho et al. (2013) emphasize the need to optimize roughing processes by precisely controlling parameters like the use of fixed abrasives, time, and platen rotation speed. Complementarily, Ohara et al. (2010) highlight the significance of evaluating the impact of these factors on surface roughness to achieve finely finished surfaces.

Surface quality and flatness are crucial factors in coating technologies, influencing the uniformity and stability of coating thicknesses (Vrbová et al., 2024). Optical flatness metrology has significantly improved over the past 40 years, with advanced techniques like interferometric three-flat tests and difference deflectometry enabling nanometer-level measurements (Schulz et al., 2008). In addition, the cleaning process, as described in ISO 27831 (2008), is essential to achieve mirror-like surfaces. The assessment of instrumental effects on measurements can be significantly improved, as suggested by Kim et al. (2007). In this context, ASTM E-3

(2017) and ISO 8504-2 (2019) standard methodologies have been employed for surface preparation, requiring a solid basis for obtaining mirror-polished metal surfaces.

The quality of the deposited coatings is highly dependent on substrate properties such as hardness, roughness, and surface defects. For example, carbides present in the substrate play a crucial role in determining its hardness. A higher ordering in the distribution of carbides represents an increase in substrate hardness (Serna et al., 2014). The main carbides present in M2 steel are M2C, which have a compact hexagonal (HCP) and orthorhombic crystal structure. While MC and M6C carbides exhibit a civic crystal structure centered on the FCC faces (Serna et al., 2009).

Padmini (2020) has shown that substrate roughness affects the wear resistance of coatings, with shot-blasted surfaces being the most promising. On the other hand, Ding (2008) has observed that substrate hardness significantly influences the toughness and adhesion of hard coatings, underlining the need for high-hardness substrates. Vladimirov (2000) has also highlighted the crucial role of substrate surface roughness in improving the wear resistance of coatings, with an optimum roughness value depending on the coating thickness.

For this reason, the surface finish of the substrate is taken as the central focus. However, the definition of the term "mirror finish" is defined according to the final application in a very specific way for each field. Given these differences, it becomes essential to define 'mirror finish' in a manner that is specific to the intended application. For instance, in fields such as electronics, optics, materials science, or metrology, the criteria for 'mirror finish' differ, although they often share the common factor of evaluating gloss as a function of surface roughness. Considering these circumstances, a proposal is made in quantitative terms on what can be considered a mirror-finished surface on substrates to be used in coating processes for various applications.

This research article evaluates the mirror finish surface quality of metallic substrates using a combination of advanced techniques including optical microscopy to identify surface defects, profilometry to detect valleys and peaks, and X-ray diffraction to evaluate the crystal structure and phases present in both, the substrate and the coating. Additionally, Field Emission Scanning Electron Microscopy (FESEM) was used to confirm the presence of carbides and analyze their elemental chemical composition. With this comprehensive approach, the aim is to improve the surface quality of the substrate, thus ensuring optimal results when applying coatings, with greater homogeneity and stability".

II. Materials and methods

2.1 Experimental study and analytical techniques.

Specimens were prepared by cutting an AISI M2 steel bar into 32 disks, each with a diameter of 25.00 mm and a thickness of 7.50 mm. The samples then underwent a mirror finishing process, which consisted of the following steps: (1) coarse grinding with abrasive paper (FEPA #180, #220, #320, and #500), (2) fine grinding with abrasive paper (FEPA #800, #1200, and #2000), and (3) a three stage polishing process using a 6.00 µm single-crystal diamond solution, followed by a 1.00 µm single-crystal diamond solution, and finally, an alumina solution with a particle size of 0.05 µm. The samples were then evaluated by different analytical techniques to assess the brightness and substrate/coating coherence. Surface brightness was evaluated based on the type and quantity of defects present on the mirror

finished surface, using light microscopy and profilometry. Coherence and properties to ensure adhesion in the system were evaluated with the number of carbides, by elemental mapping, X-ray diffraction, and hardness. Table 1 provides a summary of the parameters used in this study, including consumables, time, and rotation speeds, associated with the roughing, cleaning, and polishing stages.

Table 1. Summary of the ad-hoc-finished surface.

Stage	Substage	Abrasive material	Time (min)	Rotation speed (rmp)
1. Plane grinding	1.1	Abrasive paper FEPA #180	12	250
	1.2	Abrasive paper FEPA #220	4	250
	1.3	Abrasive paper FEPA #320	4	250
	1.4	Abrasive paper FEPA #500	4	250
Cleaning process (water + acetone / water + isopropyl alcohol) and pressurized air drying				
2. Fine grinding	2.1	Abrasive paper FEPA #800	4	300
	2.2	Abrasive paper FEPA #1200	5	300
	2.3	Abrasive paper FEPA #2000	6	350
Cleaning process (water + acetone / water + isopropyl alcohol) and pressurized air drying				
3. Final polishing	3.1	Cotton cloth + monocrystalline diamond suspension (6 µm)	5	300
	3.2	Cotton cloth + monocrystalline diamond suspension (1 µm)	5	300
Ultrasonic bath cleaning process (water + acetone/water + isopropyl alcohol) and pressurized air drying				

* Federation of European Producers of Abrasives (FEPA).
* Cleaning processes help to remove residues that can generate surface defects in fine polishing stages.

2.2 Light microscopy

A Nikon Epiphot 200 metallographic microscope, equipped with Axis software, was utilized to analyze the surface defects on an AISI M2 steel substrate. Prior to examination, the samples underwent a thorough cleaning process using an ultrasonic bath. The cleaning process consisted of immersing the samples in a water/acetone solution (25/75 ratio) for 10 minutes, followed by a water/isopropanol (reagent-grade) solution (25/75 ratio) for an additional 10 minutes. The samples were then dried using compressed air. To obtain the photomicrographs, bright field, and dark field illumination modes were employed to highlight specific defects, such as porosities, scratches, and comet tails, at varying magnifications in several areas of interest.

2.3 Profilometry

The contact profilometry test was conducted using a high-precision BRUKER Dektak XT profilometer, which was equipped with a sapphire probe and Vision64 software. Prior to profilometry, the sample surfaces were carefully inspected to ensure the removal of any residual contamination or moisture

through an appropriate cleaning procedure. After the cleaning procedure, 5.00 x 5.00 mm area scans were performed on several areas of interest on the surface, covering at least 80.00 % of the sample. The objective of these scans was to observe the distribution of roughness and texture along the surface. For this purpose, high precision and accuracy scanning was performed using Vision64 software algorithms to capture and analyze detailed topographic data.

2.4 X-ray Diffraction Analysis

The identification of the phases and crystalline structures present in the substrate and coating was performed using the Rigaku SmartLab X-ray diffraction (XRD) equipment. For the acquisition of data, the surfaces of five samples of both the substrate and coating were analyzed using the SmartLab guidance software and the iCDD database. The XRD was operated at a voltage of 50 kV and a current of 54 mA in the X-ray tube.

2.5 Scanning Electron Microscopy and EDS

Scanning electron microscopy (SEM) was used to identify surface defects smaller than 1.00 μm, as well as to analyze the microstructure and perform second-phase analysis. A JEOL JSM 7200F field emission scanning electron microscope (FESEM) with Energy Dispersion X-ray Spectrometer and Aztec software was used. The analysis was obtained from the photomicrographs with secondary electrons, backscattered electron modes, and elemental maps. Photomicrographs were taken at various magnifications to specify a detail of the surface features.

2.6 Indentation test

Prior to the indentation test, the samples underwent a cleaning process, which is crucial to minimize contamination that could introduce noise in the measurements. Vickers microhardness tests were performed using Anton Paar's RST 3 instrument to determine the hardness of the samples. The microhardness tests were realized using a Vickers diamond pyramid indenter with a load of 50.00 N and a test time of one minute for each measurement. Following this procedure, five hardness measurements were realized in different areas of the surface of interest for each sample tested.

III. Results

With the different results obtained, a correlation exercise was carried out to evaluate the brightness as a measure of flatness and mirror finish, in addition to having an overview of the coherence between the mechanical and crystalline properties of the substrate and the coating.

3.1 Light microscopy

Photomicrographs analyzed in this study were obtained using both bright-field and dark-field observation modes, capturing surface views of the samples both before and after polishing. Therefore, the surface brightness can be evaluated by evaluating the number of imperfections, since these defects can cause various physical phenomena that eliminate or deflect the light decreasing the intensity observed. To obtain the data, 5 samples were selected from the 32 AISI M2 steel discs batch and analyzed by optical microscopy (Figure 1 A-B). The analyses were performed on areas of 1 500.00 μm2. The photomicrographs analyzed in this study were obtained using bright-field and dark-field observation modes, surface view of the samples, both unpolished and after polishing. Figure 1 (C-D) observed the surface to 200X.

It is important to note that a mirror finish refers to the surface’s ability to reflect light and that imperfections on the surface impact this property. Therefore, it is crucial to

minimize these defects, such as scratches, through mechanical polishing processes.

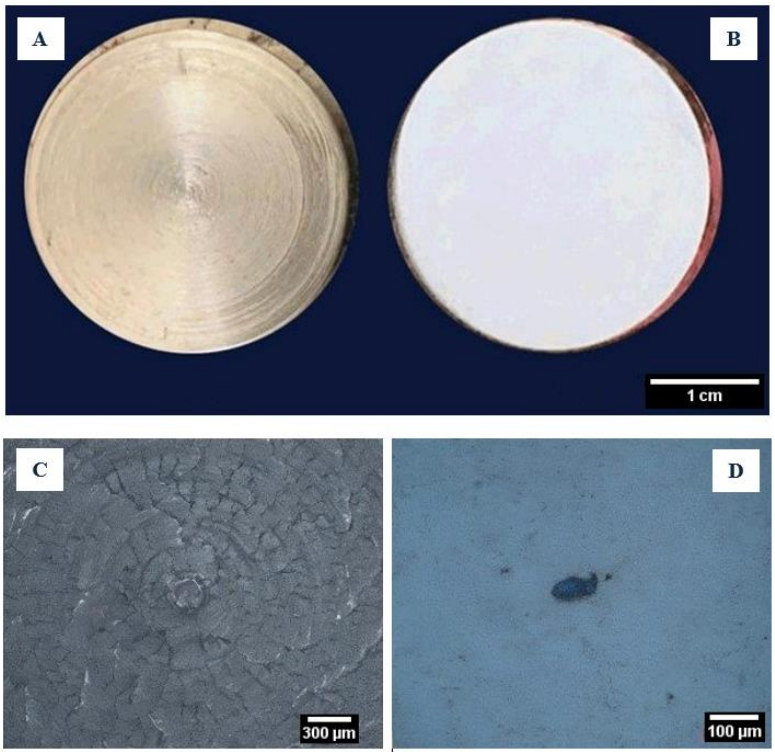

Figure 1 (A-B). Surface morphology of a sample without mirror finish and another with fine finish. **Figure 1(C-D)** presents the surface at 200X magnification.

In the upper part of Figure 2, there is a brightfield photomicrograph of the polished surface subjected to analysis for the presence of imperfections. The photomicrographs reveal the presence of surface porosity (A), scratches (B), precipitates (second phases) (C), and finely aligned precipitates (D). The results for each type of defect represent the average of the measurements made on these samples. One potential problem that can arise during the polishing process is the formation of defects known as "comet tails". These defects can occur when polishing is performed in only one direction, as well as when carbides detach from the surface, leaving trails that resemble comets (E).

Figure 2 presents a detailed view of the defects (Defects in graph A, B, C, D, E) present on the surface of the sample. To define specific criteria for the identification of the different defects, the defects with the largest size on the surface were considered. These included comet tails 10.00 µm in length, pores 1.00 µm in diameter, and cracks or scratches 20.00 µm in length.

The data presented in Figure 2 indicates insight into the nature and extent of defects present on the polished surface. In addition, the graph illustrates the relative contribution of the main imperfections observed on the ad hoc polished surfaces considered. These values can be considered as criteria for determining the degree of ad hoc finish obtained with a conventional grinding and polishing process. These results also supply information on the repeatability and reproducibility of the process used to prepare the polished surface.

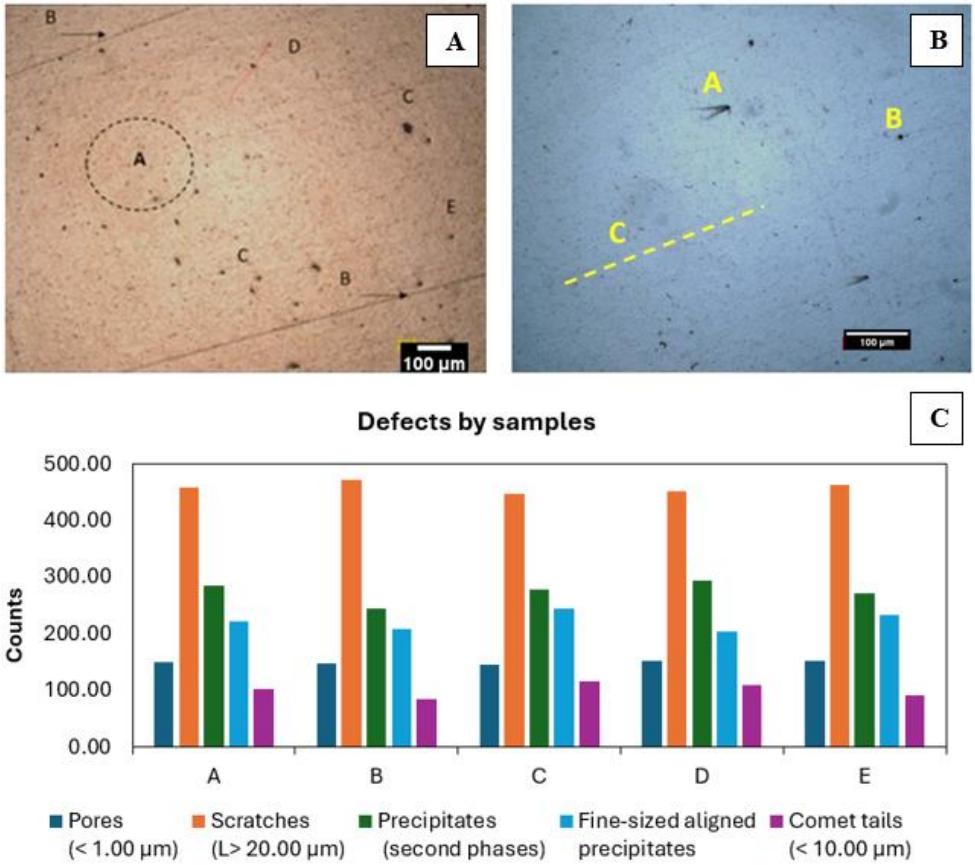

Figure 2 (A-B). Defects and imperfections analysis on a mirror-finished surface. **Figure 2 (C).** The photomicrograph presents the types of defects found, while the graph and table present information about r and R test information.

The profilometer was used to obtain information on the effect of imperfections in larger regions to complement the information obtained by microscopy. Figure 3A presents the roughness results of the untreated sample, while Figure 3B presents the roughness profile of the mirror-finished surface. The analysis results, as illustrated in Figures 3A and 3B, were used to construct a three-dimensional representation (Figure 3C and Figure 3D, below). This representation allows for a more comprehensive analysis of the substrate's characteristic valleys and peaks. In surface analysis, an untreated surface is typically expected to exhibit abrupt changes in signal, while a polished surface should exhibit smooth profiles. The results for the untreated surface are for the ridge between 1.20 and 1.50 µm, while the valley, with a value of 1.00 to 0.8 µm. The mirror-finished sample shows values for the ridge from 0.04 to 0.08 µm and for the valley from 0.04 to 0.08 µm. In the 3D view, the surface roughness can be analyzed using a color code in which the flatter regions are green, the peaks red, and the valleys blue. These results provide valuable insight into the surface morphology of the polished sample, demonstrating the effectiveness of the polishing process in producing a smooth surface. Depending on the available means, the receiving surface exhibits adequate roughness levels to achieve uniform thicknesses from the onset of deposition.

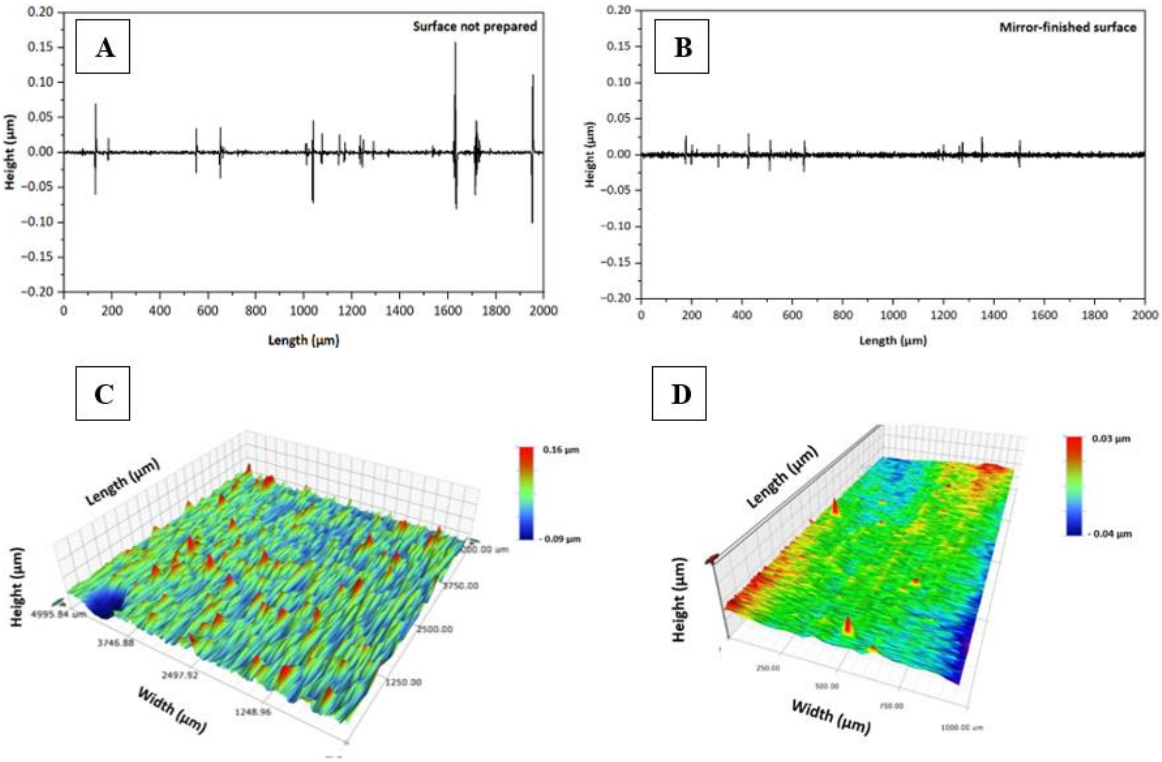

Figure 3 (A-B). The roughness profile of the surface with and without treatment is presented. **Figure 3 (C-D).** Three-dimensional representations of surface roughness profiles with and without mirror finish.

3.2. X-ray Diffraction Analysis

Another crucial aspect in achieving a uniform, stable, and homogeneous coating is ensuring that the substrate and coating system have compatible mechanical and structural properties. Coherence between these components can enhance adhesion and prevent the formation of an undesirable interface layer, which could negatively impact the performance of the fabricated material. Therefore, the system between substrate and coating is expected to achieve harmony between their crystal lattices. X-ray diffraction (XRD) analysis was used to identify the crystalline structure and phases present in the titanium coating and M2 steel (Figure 4A). For titanium, the characteristic peaks correspond to the alpha (α) and beta (β) phases (Figure 4B): alpha phase (Hexagonal Close-Packed, HCP) shows peaks at 35.1° (002) and 38.4° (100), while the beta phase (Body Centered Cubic, BCC) shows peaks at 39.2° (110) and 56.6° (200).

And, for M2 steel, peaks associated with iron phases such as austenite (face-centered cubic, FCC) and carbides are present (which may vary according to their elemental chemical composition). Moreover, the main carbides present in M2 steel, MC, and M_6C (Serna et al., 2009) have an FCC crystalline structure like that of the substrate, therefore, the presence of carbides on the substrate surface increases the coherence between the system formed by the substrate and the coating, improving the adhesion between them.

The alpha (HCP) and beta (BCC) phases of titanium affect the hardness and adhesion of the coating. The presence of FCC-structured carbides in M2 steel provides additional anchor points that improve adhesion between the substrate and the coating. Identifying characteristic peaks in a diffraction pattern allows us to ascertain the phases present and detect any defects, internal stresses, or

impurities. The alignment of peaks between the coating and substrate indicates compatible crystal structures, which enhances adhesion and minimizes internal stresses. Structural and chemical compatibility between the coating and substrate phases, such as the alpha and beta phases of titanium and austenite in M2 steel, improves adhesion and provides an optimal balance of strength and toughness, which is essential for applications in extreme conditions.

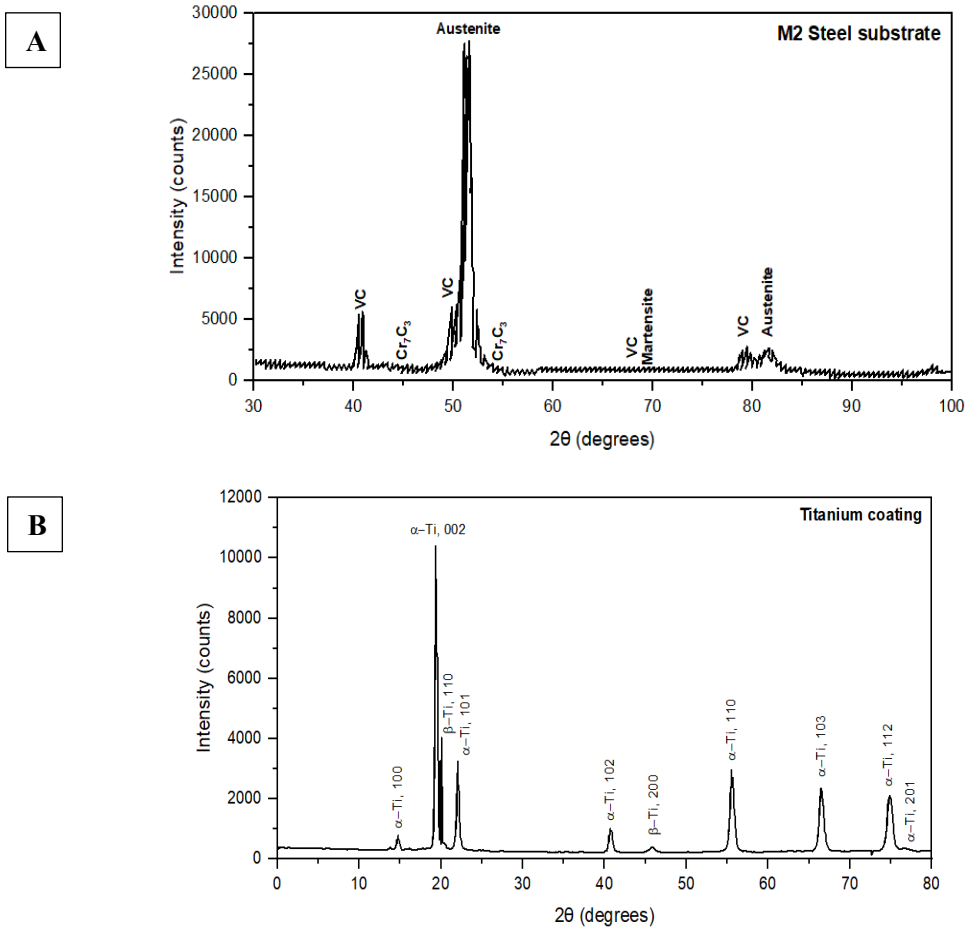

Figure 4A. The diffractogram of the substrate confirms the presence of austenite in greater quantity with an FCC type crystalline structure. **Figure 4B.** The diffractogram of the coating confirms the presence of the α-Ti structure, which presents an HCP type structure.

3.3 Scanning Electron Microscopy and EDS

Figure 5A presents a scanning electron microscopy (SEM) photomicrograph of the distribution of carbides on the surface of AISI M2 steel. In it we can observe a homogeneous distribution of this phase on the surface, although different sizes of carbides coexist, allowing the smaller ones to detach during the processes of preparation of the mirror surface, giving rise to the defect "comet tails".

Figure 5B presents an image of the system using backscattered electron (BSE) imaging, showing no distinct interface between the coating and substrate, indicating direct contact. Additionally, different shades within the carbides are observed, but these variations do not provide information about chemical composition profiles.

Consequently, the observed differences in chemical composition suggest differences in the crystalline structure of the carbides, which may lead to variations in the mechanical properties of these phases and influence their contribution during the surface preparation process.

Additionally, surface roughness is influenced by the chemical differences between the matrix and the individual solutes (identified carbides). Figures 6A and 6B show the location and quantification of defects analyzed by SEM-EDS. A thorough assessment of primary defects was conducted, including pores, microcracks, and carbides smaller than 0.50 µm. The presence of these defects can significantly impact the mechanical and physical properties of the material, making accurate identification and quantification crucial.

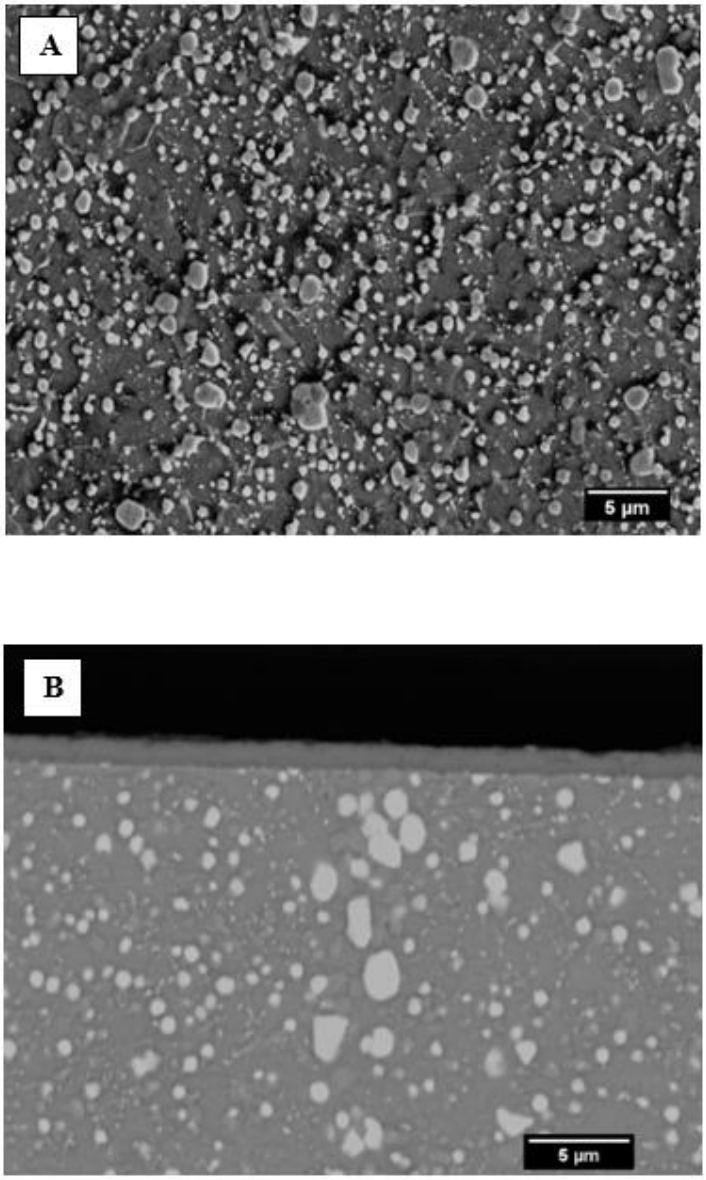

Figure 5A. Secondary electron photomicrography of the substrate surface. **Figure 5B.** Backscattered electron photomicrograph showing the carbides in the M2 steel matrix and the coating on the substrate.

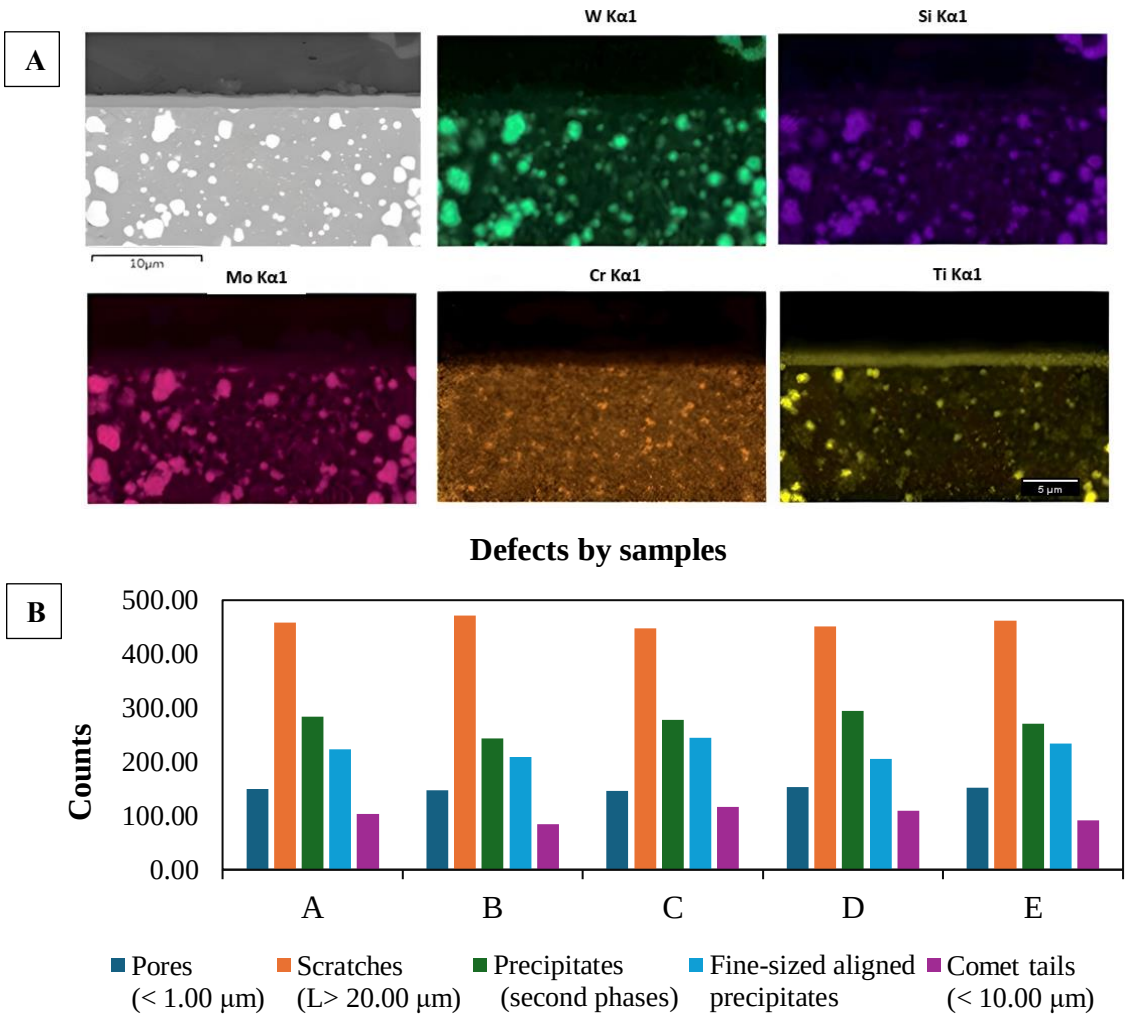

Figure 6A. EDS mapping for the identification of the elemental chemical composition of carbides present in the substrate. **Figure 6B.** Comparative plot of defects located in randomly selected samples.

3.4 Indentation test

Surface microhardness was quantified before (Figure 7A) and after polishing (Figure 7B) using identical test parameters. After examination, it was observed that the ad hoc polished surface exhibited traces suitable for analysis, while the unpolished surface lacked a well-defined pattern. This discrepancy may be the origin of the observed difference in hardness values, as illustrated in Figure 7C. Hardness is a mechanical property that provides an overview of the elastoplastic behavior of the material. An accurate determination of this property will help to discuss the behavior of the material under specific loading or deformation conditions.

The microhardness values for the untreated samples were approximately 1.50 times higher than those for the polished surface. Comparing these results with reference values from www.mat-web.com, the polished sample's hardness was consistent with the indicated values. Microhardness measurements were conducted on various regions of the surface and across different disks, both with and without surface preparation.

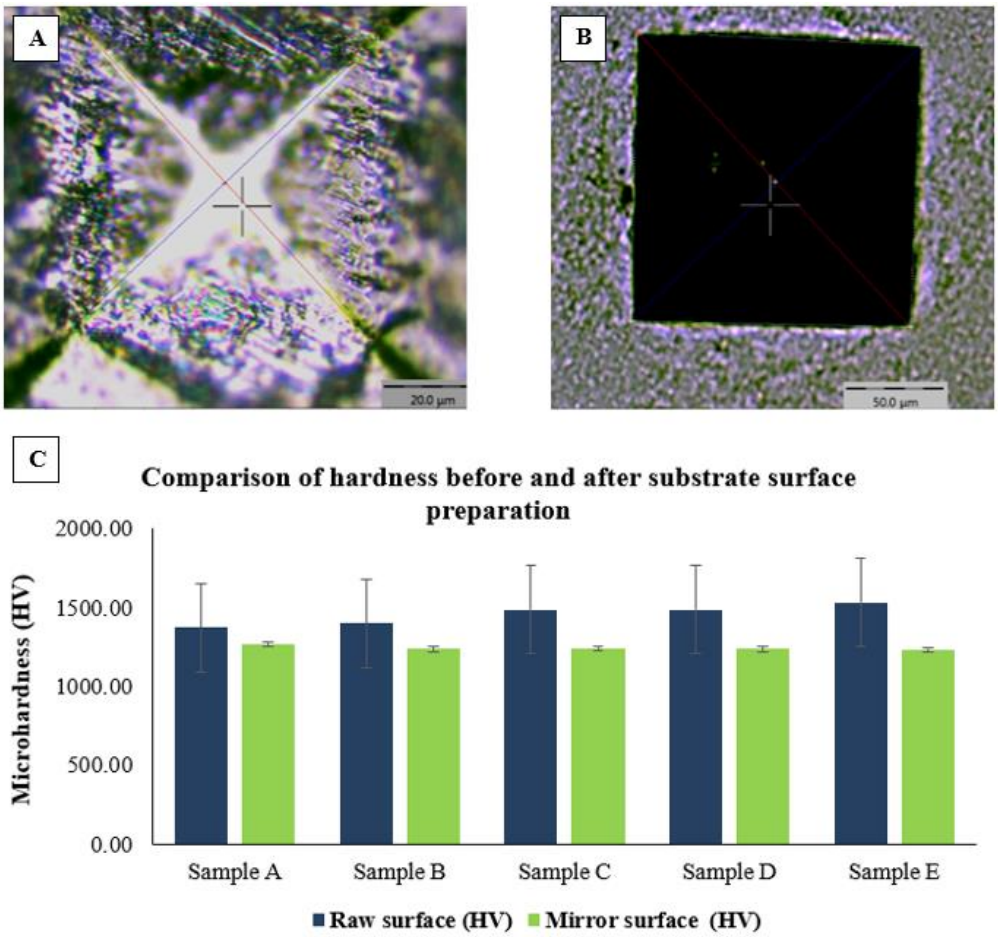

Figure 7A. Vickers indenter track on the untreated surface. **Figure 7B.** Vickers indenter track on the surface of the substrate with a mirror finish. **Figure 7C.** Comparative graph of the variation of the hardness measured on the surface of the substrate with and without treatment.

IV. Conclusions

The procedure developed in this study represents a novel technical approach to obtaining a mirror-finished surface, which represents the reduction of surface defects and imperfections. This procedure was applied to different samples, and the results were found to be repeatable, with surfaces presenting a similar appearance. The preparation of these surfaces allowed for a detailed study of the defects in the material, including pores, cracks, and comet tails, as described in the study carried out by light microscopy and profilometry.

Furthermore, it was observed that the fine polishing process was unable to remove scratches that were considered insignificant to the effects of the coating, as evidenced by images obtained by scanning electron microscopy. Elemental mapping was employed to observe the distribution of the defects and their correlation with the carbides and M2 steel matrix. It was determined that the defects did not affect the microstructure of the prepared surface. XRD verified the crystal structure of the substrate and coating. The substrate has an FCC structure, while the coating has an HCP structure. Both structures exhibit similar characteristics, allowing the system to achieve high levels of adhesion and coherence, thus facilitating the formation of homogeneous and stable coatings. No interface was identified within the system.

The crystal structures of titanium (coating) and M2 steel (substrate) present a high degree of thermodynamic coherence due to the following similarities:

- Both structures exhibit a high atomic density with a packing fraction of 74%. The coordination number is the same in both structures, being 12 atoms for each structure.
- The directions of highest atomic concentration are different, being the edges of the bases of the hexagonal prism in the HCP structure and the diagonals of the face in the FCC structures. However, this does not significantly affect the thermodynamic stability.
- The planes of highest atomic concentration are parallel to the hexagonal prism bases and parallel to the cube faces in the FCC structure.

It is crucial to define the intended use of the coating in order to guarantee that the characteristics of the substrate are accurately transferred to the coating. A uniform, homogeneous, and stable coating provides superior properties and increased durability compared to heterogeneous coatings. This method is therefore a preferred choice for demanding industrial and technological applications.

V. References

1. Altenburg, S.J., Weber, H.P., Krankenhagen, R. (2017) "Thickness determination of semitransparent solids using flash thermography and an analytical model", *Quantitative InfraRed Thermography*, 15(1), pp. 95-105. https://doi.org/10.1080/17686733.2017.1331655.

2. ASTM E3-11. (2017). *Standard Guide for Preparation of Metallographic Specimens*.

3. Cho, B.-J. et al. (2013) "On the mechanism of material removal by fixed abrasive lapping of various glass substrates", *Wear*, 302(1-2), pp. 1334-1339. https://doi.org/10.1016/j.wear.2012.11.024.

4. D'Agostino, A.T. (1994) "A multi-technique approach for materials characterization: using X-Ray diffractometry, visible spectroscopy, and atomic absorption analysis to determine thin metal film thickness", *Journal of Chemical Education*, 71(10), p. 892. https://doi.org/10.1021/ed071p892.

5. Habib, S.J. y Okada, A. (2016) "Study on the movement of wire electrode during fine wire electrical discharge machining process", *Journal of Materials Processing Technology*, 227, pp. 147-152. https://doi.org/10.1016/j.jmatprotec.2015.08.015.

6. Harrison, R.W. (1943) "Standard costing of plating processes", *Transactions of the IMF*, 19(1), pp. 91-105. https://doi.org/10.1080/00202967.1943.11869421.

7. Heng, L., Kim, Y.J. y Mun, S.D. (2017) "Review of superfinishing by the Magnetic Abrasive Finishing Process", *High-Speed Machining*, 3(1). https://doi.org/10.1515/hsm-2017-0004.

8. International Organization for Standardization. (2008). *Metallic and other inorganic coatings - Cleaning and preparation of metal surfaces* (ISO 27831).
9. International Organization for Standardization. (2018). *Road vehicles -*

Cleanliness of components and systems (ISO 16232).

10. Kasuriya, P. et al. (2022) “Mirror surface finishing of hardened stainless steel using spherical PCD tool”, *Precision Engineering*, 74, pp. 163-174. https://doi.org/10.1016/j.precisioneng.2021.11.003.

11. Kim, J., Pierron, F., Grediac, M., & Wisnom, M. R. (2007). A Procedure for Producing Reflective Coatings on Plates to be Used for Full-Field Slope Measurements by a Deflectometry Technique. Strain, 43(2), 138-144. https://doi.org/10.1111/j.1475-1305.2007.00324.x.

12. Kuhar, M. y Funduk, N. (2005) “Effects of polishing techniques on the surface roughness of acrylic denture base resins”, *Journal of Prosthetic Dentistry*, 93(1), pp. 76-85. https://doi.org/10.1016/j.prosdent.2004.10.002.

13. Martinuzzi, S. et al. (2021) “A robust and cost-effective protocol to fabricate calibration standards for the thickness determination of metal coatings by XRF”, *Spectrochimica Acta Part B: Atomic Spectroscopy*, 182, p. 106255. https://doi.org/10.1016/j.sab.2021.106255.

14. Ohara, K. et al. (2010) “Numerical analysis of film thickness of electrodeposited paint coating for the whole automotive body using virtual surface”, *Transactions of the IMF*, 88(6), pp. 294-302. https://doi.org/10.1179/174591910x12838729735387.

15. Pennisi, M.S. (1988b) “The control of quality in metal finishing operations”, *Transactions of the IMF* [Preprint]. https://doi.org/10.1080/00202967.1988.11870807.

16. Rudjord, Ø., et al. (2022) “Estimating thin ice thickness around Svalbard using MODIS satellite imagery”, *Geografiska Annaler: Series A, Physical Geography*, 104(2), pp. 127-149. https://doi.org/10.1080/04353676.2022.2070158.

17. Schaffer, M., Schaffer, B. y Ramasse, Q.M. (2012b) “Sample preparation for atomic-resolution STEM at low voltages by FIB”, *Ultramicroscopy*, 114, pp. 62-71. https://doi.org/10.1016/j.ultramic.2012.01.005.

18. Schulz, M., Wiegmann, A., Márquez, A., & Elster, C. (2008). Optical flatness metrology: 40 years of progress Metrología óptica de superficies planas: 40 años de progreso. https://www.semanticscholar.org/paper/Optical-flatness-metrology%3A-40-years-of-progress-de-Schulz-Wiegmann/93431f15060f881252b6505616c38885944e3e8e#citing-papers.

19. Townsend, A. et al. (2016) “Surface Texture Metrology for Metal Additive Manufacturing: A review”, *Precision Engineering*, 46, pp. 34-47. https://doi.org/10.1016/j.precisioneng.2016.06.001.

20. Upton, D.P. (1990) 'The performance of new PVD coatings on cutting tools', *Transactions of the IMF*, 68(4), pp. 118-120. https://doi.org/10.1080/00202967.1990.11870880.

21. Vrbová, H., Kubišová, M., Pata, V., Knedlová, J., Javořík, J., & Bočáková, B.

(2024). Approach to Heterogeneous Surface Roughness Evaluation for Surface Coating Preparation. Coatings, 14(4), 471. https://doi.org/10.3390/coatings14040471.